

## Fingerprinting the Phases of Thin Film Ge<sub>2</sub>Sb<sub>2</sub>Te<sub>5</sub> with EELS

Ho Leung Chan<sup>1</sup>, Matthew Mecklenburg<sup>2</sup>, William Hubbard<sup>3</sup>, Jared Lodico<sup>1</sup>, Brian Zutter<sup>1</sup> and B. C. Regan<sup>4</sup>

<sup>1</sup>University of California, Los Angeles, Los Angeles, California, United States, <sup>2</sup>University of Southern California, Los Angeles, California, United States, <sup>3</sup>NanoElectroning Imaging, Inc. (NEI), Los Angeles, California, United States, <sup>4</sup>Department of Physics & Astronomy, University of California-Los Angeles, Los Angeles, California, United States

Phase change memory (PCM) is an attractive next-generation, non-volatile data storage technology. Ge<sub>2</sub>Sb<sub>2</sub>Te<sub>5</sub> (GST), a ternary chalcogenide phase change material, is a promising candidate PCM material that exhibits three distinct structural phases and a resistivity that changes with temperature and phase over more than five orders of magnitude [1]. In PCM high- and low-resistance states are used to encode the binary values “0” and “1”, respectively. Although the concept of using chalcogenides as PCM was first proposed over 50 years ago [2], only recently has PCM become a commercial product available on the marketplace, where it is beginning to compete with the now more prevalent flash memory [3]. Here, we use scanning transmission electron microscopy (STEM) and electron energy loss spectroscopy (EELS) to identify and observe the thermally induced phase transitions in a GST thin film.

Our *in situ* heating-biasing chip has a heater, which is isolated from the rest of the sample by a layer of 7 nm ALD alumina, and a pair of biasing probes that are fabricated on an electron transparent Si<sub>3</sub>N<sub>4</sub> membrane. The Ti/Pt (5/25 nm) heater and probes are patterned via e-beam lithography. A 30 nm blanket film of GST, which is amorphous as deposited, is sputtered over the testbed to complete the device (Fig. 1). As the bias voltage on the heater increases, the GST begins to transition from its amorphous phase (Fig. 1B) to the fcc phase (Fig. 1C). The fcc phase consists of small (~5 nm), randomly oriented crystallites. Further increasing the temperature on the GST film causes it to transition into its hexagonal phase (Fig. D), which has bigger (~200 nm) crystalline grains. The resistance between the probes changes from ~800 MΩ to ~200 kΩ to ~30 kΩ as the film goes from as-deposited to fcc to hexagonal, respectively.

Low-loss EELS spectra across the three different GST phases (Fig. 2A-C) are acquired with a Gatan Quantum SE spectrometer in a JEOL JEM-2100F microscope operating at 80 kV. In the upper left corner of the scan region, the GST is amorphous, as indicated by the uniform ADF STEM contrast (Fig. 2A). In the center of the scan region the GST is in the fcc phase, while the material nearest the heater is in the hexagonal phase (Fig. 2A). EELS spectra (Fig. 2D) integrated over three regions show that the plasmon energy shifts up through  $16.33 \pm 0.03$ ,  $16.45 \pm 0.04$ , and  $16.49 \pm 0.04$  eV (Fig. 2D inset) when the film is in the amorphous, fcc, and hexagonal phases, respectively. Significant, systematic plasmon energy shifts are present within the fcc phase (see gradient around the green box in Fig. 2C). While the plasmon energy shifts agree qualitatively with the corresponding densities of 5.87, 6.27, and 6.39 g/cm<sup>3</sup> [4], they are about four times smaller than the naive expectation. Further study is necessary to reveal the subtler features of the relationships between the GST phase and the measured plasmon energies [5].

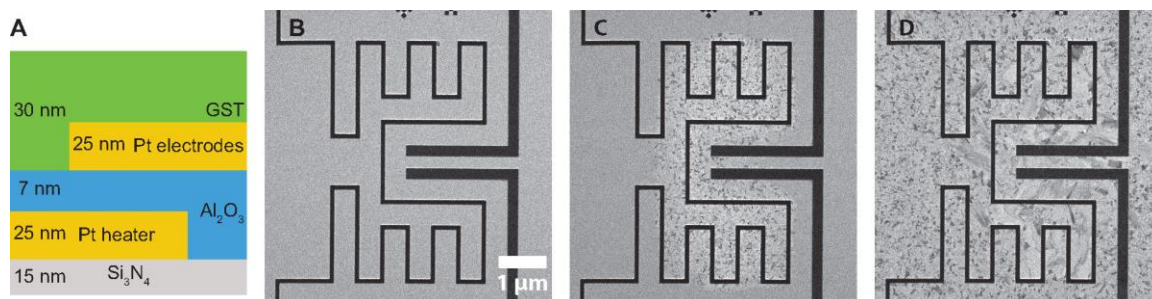


**Figure 1. Schematic device cross-section (A) and time series of BF STEM images of GST undergoing phase change (B-D).** The device consists of an electron transparent  $\text{Si}_3\text{N}_4$  membrane, a Pt heater, a layer of ALD  $\text{Al}_2\text{O}_3$ , a pair of Pt electrodes, and a thin film of GST. The GST is amorphous (B) as deposited. It changes from amorphous to fcc (C) to hexagonal (D) as the heater power is increased.

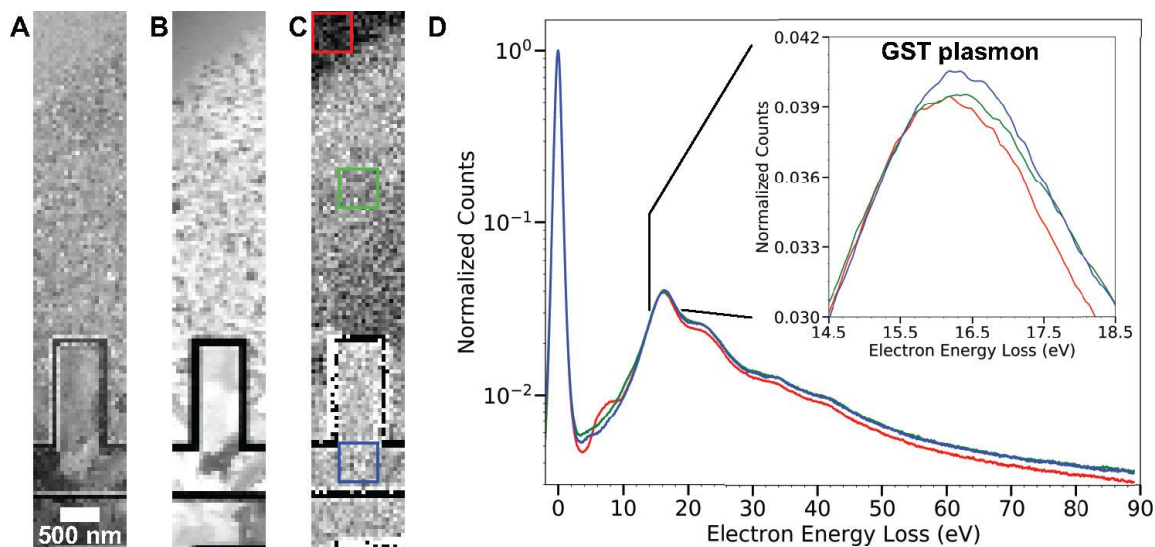


**Figure 2. ADF STEM image (A), energy filtered image (B), plasmon energy map (C), and the low-loss EELS spectra (D) of GST.** The energy filtered image (B) shows the integrated intensity in the energy range 14.5 - 18.5 eV, which captures most of the plasmon signal. The EELS spectra (D) are integrated over the three regions indicated by the three colored boxes: amorphous (red), fcc (green), and hexagonal (blue). The inset shows the GST plasmon energy shift, and the spectra have been normalized relative to the maximum of the zero-loss peak.

## References

- [1] GW Burr et al., *Journal of Vacuum Science & Technology B* **28** (2010), p. 223–262.
- [2] SR Ovshinsky, *Phys. Rev. Lett.* **21** (1968), p. 1450–1453.
- [3] H-S P Wong et al., *Proceedings of the IEEE* **98** (2010), p. 2201–2227.
- [4] WK Njoroge et al., *Journal of Vacuum Science & Technology A* **20** (2002), p. 230–233.
- [5] This work was supported by SRC NMP 2872.001, NSF STC award DMR-1548924 (STROBE), and NSF award DMR-1611036. Data presented here were acquired at the Core Center of Excellence in Nano Imaging (CNI) at the University of Southern California.